HHS Public Access

Author manuscript

Oncogene. Author manuscript; available in PMC 2017 January 06.

Published in final edited form as:

Oncogene. 2017 February 02; 36(5): 687–699. doi:10.1038/onc.2016.240.

Interleukin-17 promotes prostate cancer via MMP7-induced epithelial-to-mesenchymal transition

Q Zhang[1,12], **S Liu**[1,12], **KR Parajuli**[1], **W Zhang**[2], **K Zhang**[2], **Z Mo**[1,3], **J Liu**[1,3], **Z Chen**[1,4], **S Yang**[1,5], **AR Wang**[6], **L Myers**[7], and **Z You**[1,8,9,10,11]

[1]Department of Structural and Cellular Biology, Tulane University, New Orleans, LA 70112, USA

[2]Department of Computer Science and Biostatistics Facility of RCMI Cancer Research Center, Xavier University of Louisiana, New Orleans, LA 70125, USA

[3]Department of Obstetrics and Gynecology, Shijiazhuang Maternal and Child Health Care Hospital, Shijiazhuang 050000, China

[4]Department of Thoracic Surgery, Affiliated Hospital of North China University of Science and Technology, Tangshan 063000, China

[5]Department of Urology, the Third Hospital of Hebei Medical University, Shijiazhuang 050011, China

[6]Department of Pathology and Laboratory Medicine, Tulane University, New Orleans, LA 70112, USA

[7]Department of Biostatistics and Bioinformatics, Tulane University, New Orleans, LA 70112, USA

[8]Department of Orthopaedic Surgery, Tulane University, New Orleans, LA 70112, USA

[9]Tulane Cancer Center and Louisiana Cancer Research Consortium, Tulane University, New Orleans, LA 70112, USA

[10]Tulane Center for Stem Cell Research and Regenerative Medicine, Tulane University, New Orleans, LA 70112, USA

[11]Tulane Center for Aging, Tulane University, New Orleans, LA 70112, USA

Abstract

Chronic inflammation has been associated with a variety of human cancers including prostate cancer. Interleukin-17 (IL-17) is a critical pro-inflammatory cytokine, which has been demonstrated to promote development of prostate cancer, colon cancer, skin cancer, breast cancer,

Correspondence: Dr. Z You, Department of Structural and Cellular Biology, Tulane University School of Medicine, 1430 Tulane Ave mailbox 8649, New Orleans, LA 70112, USA. Tel: 001 504 988 0467; FAX: 001 504 988 1687; zyou@tulane.edu.

[12]Co-first author.

CONFLICT OF INTEREST

The authors declare no conflict of interest.

Supplementary Information accompanies the paper on the Oncogene website (http://www.nature.com/onc): Supplementary Figures S1 and S2 present additional pictures of immunohistochemical staining, Figure S3 presents data from PC-3 cells, and Table S1 presents PCR primer sequences.

lung cancer, and pancreas cancer. IL-17 promotes prostate adenocarcinoma with a concurrent increase of matrix metalloproteinase 7 (MMP7) expression in mouse prostate. Whether MMP7 mediates IL-17's action and the underlying mechanisms remain unknown. We generated *Mmp7* and *Pten* double knockout (*Mmp7*$^{-/-}$ in abbreviation) mouse model and demonstrated that MMP7 promotes prostate adenocarcinoma through induction of epithelial-to-mesenchymal transition (EMT) in *Pten*-null mice. MMP7 disrupted E-cadherin/β-catenin complex to up-regulate EMT transcription factors in mouse prostate tumors. IL-17 receptor C and *Pten* double knockout mice recapitulated the weak EMT characteristics observed in *Mmp7*$^{-/-}$ mice. IL-17 induced MMP7 and EMT in human prostate cancer LNCaP, C4-2B, and PC-3 cell lines, while siRNA knockdown of MMP7 inhibited IL-17-induced EMT. Compound III, a selective MMP7 inhibitor, decreased development of invasive prostate cancer in *Pten* single knockout mice. In human normal prostates and prostate tumors, *IL-17* mRNA levels were positively correlated with *MMP7* mRNA levels. These findings demonstrate that MMP7 mediates IL-17's function in promoting prostate carcinogenesis through induction of EMT, indicating IL-17-MMP7-EMT axis as potential targets for developing new strategies in the prevention and treatment of prostate cancer.

Keywords

IL-17; MMP7; epithelial-to-mesenchymal transition; prostate cancer

INTRODUCTION

Chronic inflammation has been associated with a variety of human cancers. Approximately 15% of all human cancers have been suggested to result from infection and chronic inflammation.[1] Almost all surgical prostate specimens contain evidence of inflammation.[2-4] Chronic inflammation invokes proliferative inflammatory atrophy of prostate – a potential precursor lesion to prostatic intraepithelial neoplasia (PIN) and carcinoma.[5] The cause of prostatic inflammation includes infection, urine reflux, diet, estrogen, and physical trauma.[6,7] Inflammation is a complex response involving many immune cells, chemokines, and cytokines as well as matrix-degrading enzymes.

Interleukin-17 (IL-17, also named IL-17A) is a key pro-inflammatory cytokine that plays critical roles in many inflammatory and autoimmune diseases.[8] IL-17 has been demonstrated to promote development of colon cancer,[9-12] skin cancer,[13,14] breast cancer,[15] prostate cancer,[16,17] lung cancer,[18,19] and pancreas cancer.[20] IL-17 is secreted by T helper 17 (T_H17) cells, γδ T cells, natural killer cells, and other immune cells.[21] IL-17 acts on IL-17RA/IL-17RC receptor complex to recruit nuclear factor-κB (NF-κB) activator 1 (Act1). Act1 activates tumor necrosis factor receptor-associated factor 6 (TRAF6),[22] and subsequently activates transforming growth factor-β-activated kinase 1 (TAK1) and IκB kinase (IKK) complex, resulting in activation of NF-κB pathway that initiates transcription of a variety of chemokines and cytokines, such as C-X-C motif ligand 1 (*CXCL1*), C-C motif ligand 20 (*CCL20*), *IL-1β*, and *IL-6*.[8] These IL-17-downstream factors promote cancer formation through increased cellular proliferation, attenuated apoptosis, and sustained angiogenesis, as well as creation of an immunotolerant microenvironment.

We have previously generated an IL-17 receptor C (*Il-17rc*) and prostate-specific conditional phosphatase and tensin homolog (*Pten*) double knockout (KO) mouse model.[16,17] IL-17RC-deficient (IL17-RC^{-} or RC^{-}) mice display smaller prostates and develop a reduced number of invasive prostate adenocarcinomas, compared to IL-17RC-sufficient (IL17-RC^{+} or RC^{+}) mice. Further, matrix metalloproteinase 7 (MMP7) expression is increased in RC^{+} mice compared to RC^{-}mice.[16] However, whether MMP7 mediates IL-17's action and the underlying molecular mechanisms remain unknown. MMP7 (also known as putative metalloproteinase I or matrilysin) is exclusively expressed in the epithelial cells.[23] MMP7 is overexpressed in human prostate cancer,[24] but not expressed in normal prostate glands.[25] Here, we investigated the role of MMP7 in mediating IL-17's action, using an *Mmp7* and *Pten* double KO mouse model. Our findings demonstrate that MMP7 mediates IL-17's function in promoting prostate carcinogenesis through induction of epithelial-to-mesenchymal transition (EMT).

EMT involves changes in epithelial cells to behave more like mesenchymal cells.[26] Cells undergoing EMT switch from a polarized epithelial phenotype to a highly mobile mesenchymal phenotype.[27] Expression of epithelial markers such as E-cadherin, claudin, and zona occludens 1 (ZO-1) is decreased, whereas expression of mesenchymal markers such as vimentin and N-cadherin is increased. EMT has been associated with cellular invasiveness[28] and cancer metastasis.[29-31]

RESULTS

MMP7 is the main active MMP in mouse prostate tumors

Mmp7 traditional KO mice[32] were crossbred with *Pten* conditional KO mice[33] to generate *Mmp7*$^{+/+}$;*Pten*$^{L/L}$;Cre^{+} (*Mmp7*$^{+/+}$ in abbreviation) mice, *Mmp7*$^{+/-}$;*Pten*$^{L/L}$;Cre^{+} (*Mmp7*$^{+/-}$ in abbreviation) mice, and *Mmp7*$^{-/-}$;*Pten*$^{L/L}$;Cre^{+} (*Mmp7*$^{-/-}$ in abbreviation) mice (Figure 1a). Male mice were genotyped at 3 weeks of age (Figure 1b). MMP7 protein in mouse prostates was confirmed by immunohistochemical (IHC) staining (Figure 1c) and Western blot (Figure 1d). To assess MMP enzyme activity in mouse prostates, MMPSense™ 750 FAST Fluorescent Imaging Agent (PerkinElmer, Inc., Waltham, MA) was injected intravenously into 30-week-old *Mmp7*$^{+/+}$ and *Mmp7*$^{-/-}$ mice. This agent is optically silent and produces fluorescent signals after cleavage by active MMPs including MMP2, 3, 7, 9, 12, and 13. The animals were scanned with IVIS® Lumina XRMS imaging system (PerkinElmer, Inc.).[34] *Mmp7*$^{+/+}$ mice, but not *Mmp7*$^{-/-}$ mice, showed MMP activities in the prostate region (Figure 1e). Scanning of the freshly dissected genitourinary blocs (GU-blocs) confirmed that the fluorescent signals came from *Mmp7*$^{+/+}$ prostates, but not *Mmp7*$^{-/-}$ prostates (Figure 1f). Together, these results indicated that MMP7 was the main active MMP in mouse prostate tumors.

Mmp7$^{-/-}$ mice develop smaller prostate tumors than *Mmp7*$^{+/+}$ *mice*

The GU-bloc weight has often been used to represent the prostate tumor burden.[16] Prostate tumors of *Mmp7*$^{+/+}$ mice were obviously larger than those of *Mmp7*$^{-/-}$ mice at 30 weeks of age (Figure 2a). At 9 weeks of age, the GU-bloc weight showed no significant differences among the three groups of animals ($P > 0.05$). However, at 30 weeks of age, the GU-bloc

weight of *Mmp7*$^{+/+}$ mice was significantly heavier than that of *Mmp7*$^{-/-}$ mice ($P < 0.05$, Figure 2b). The GU-bloc weight of *Mmp7*$^{+/-}$ mice was slightly heavier than that of *Mmp7*$^{-/-}$ mice ($P > 0.05$, Figure 2b). These results indicated that *Mmp7*$^{-/-}$ mice developed smaller prostate tumors than *Mmp7*$^{+/+}$ mice.

Mmp7 KO decreases formation of invasive prostate adenocarcinoma

We and other researchers have reported that *Pten*$^{L/L}$;*Cre*$^{+}$ mice develop invasive prostate adenocarcinoma at 9 weeks of age.[16,33] Here, we found that invasive prostate adenocarcinomas were formed at different rates among *Mmp7*$^{+/+}$, *Mmp7*$^{+/-}$, and *Mmp7*$^{-/-}$ mouse prostates at 9 and 30 weeks (Figures 2c and d). At 30 weeks of age, 33% and 27% of prostatic glands presented with invasive prostate adenocarcinomas in *Mmp7*$^{+/+}$ and *Mmp7*$^{+/-}$ mice, respectively. In contrast, only 11% of prostatic glands showed invasive prostate adenocarcinomas in *Mmp7*$^{-/-}$ mice. The differences in the percentages of lesions were statistically significant between *Mmp7*$^{+/+}$ and *Mmp7*$^{-/-}$ mice at 9 and 30 weeks and between *Mmp7*$^{+/-}$and *Mmp7*$^{-/-}$ mice at 30 weeks ($P < 0.01$, Figure 2d). These results suggested that *Mmp7* KO decreased formation of invasive prostate adenocarcinoma.

Mmp7 KO decreases cellular proliferation and increases apoptosis in the prostate lesions

To reveal the underlying cause of the differences in prostate tumor burden among the animals at 30 weeks of age, we found that there were significantly more Ki-67-positive cells in *Mmp7*$^{+/+}$ and *Mmp7*$^{+/-}$prostates than in *Mmp7*$^{-/-}$prostates ($P < 0.05$ or 0.01, Figures 3a and b). In addition, there were significantly fewer apoptotic cells in *Mmp7*$^{+/+}$ and *Mmp7*$^{+/-}$ prostates than in *Mmp7*$^{-/-}$ prostates ($P < 0.05$ or < 0.01, Figures 3c and d). These results suggested that the decreased prostate tumor burden in *Mmp7*$^{-/-}$ mice was due to decreased cellular proliferation and increased apoptosis in mouse prostates.

Mmp7 KO decreases angiogenesis in the prostate lesions

MMP7 has been associated with angiogenesis through stimulating proliferation of endothelial cells in human colon cancer[35] and human umbilical vein endothelial cells,[36] thus we assessed angiogenesis in mouse prostate tumors using IHC staining of CD31. We found that there were significantly more blood vessels in *Mmp7*$^{+/+}$ prostates than in *Mmp7*$^{+/-}$ or *Mmp7*$^{-/-}$ prostates ($P < 0.05$), which was accompanied with higher levels of vascular endothelial growth factor A (VEGFA) in *Mmp7*$^{+/+}$ prostates than in *Mmp7*$^{+/-}$ or *MmpP7*$^{-/-}$ prostates (Figures 3e to h). These results indicated that reduced VEGFA expression and angiogenesis in *MMP7*$^{-/-}$ prostates contributed to the decreased prostate tumor burden in *MMP7*$^{-/-}$ mice.

Mmp7 KO inhibits epithelial-to-mesenchymal transition (EMT) in the prostate lesions

To further understand the molecular mechanisms underlying the reduced prostate tumor formation in *Mmp7* KO mice, we examined expression of several epithelial and mesenchymal marker proteins in the prostate lesions. We found that *Mmp7*$^{-/-}$ mice had obviously increased expression of epithelial markers such as E-cadherin, claudin, and ZO-1, compared to *Mmp7*$^{+/+}$ and *Mmp7*$^{+/-}$ mice (Figures 4a and b; and Supplementary Figure S1f). In contrast, *Mmp7*$^{-/-}$ mice had reduced expression of mesenchymal markers such as β-

catenin, vimentin, and N-cadherin, compared to *Mmp7*$^{+/+}$ and *Mmp7*$^{+/-}$ mice (Figures 4c and d; and Supplementary Figure S1e). Western blot analysis of the prostate tissue proteins confirmed the IHC results (Figure 4e). Since EMT is induced by certain transcription factors such as Snail, Slug, Twist, and ZEB1, we also assessed their expression levels. We found that the expression levels of Snail, Slug, Twist, and ZEB1 were reduced in *Mmp7*$^{-/-}$ prostates, compared to *Mmp7*$^{+/+}$ and *Mmp7*$^{+/-}$ prostates (Supplementary Figures S1a to d). Together, these results suggested that *Mmp7*$^{+/+}$ and *Mmp7*$^{+/-}$ prostates showed higher expression levels of mesenchymal markers and transcription factors, whereas *Mmp7*$^{-/-}$ prostates showed higher expression levels of epithelial markers, implying that *Mmp7* KO weakened EMT characteristics in the mouse prostate tumors.

MMP7 induces EMT by disrupting E-cadherin/β-catenin complex

E-cadherin interacts with a β-catenin-based complex to act on actin cytoskeleton and mediate adhesion-dependent signaling, and several proteinases including MMP7 are known to be able to cleave E-cadherin.[37-39] Thus, we tested if MMP7 could cleave E-cadherin in three human prostate cancer cell lines LNCaP, C4-2B, and PC-3. We generated MMP7-overexpressing cell lines LNCaP-MMP7, C4-2B-MMP7, and PC-3-MMP7. We observed that LNCaP-MMP7 and C4-2B-MMP7 cells appeared like mesenchymal (spindle-shaped) cells, whereas the parental LNCaP and C4-2B cells appeared like epithelial (cobblestone-like) cells (Figures 5a to d). In addition, E-cadherin staining changed from cytoplasmic membrane localization in LNCaP and C4-2B cells to cytoplasmic localization in LNCaP-MMP7 and C4-2B-MMP7 cells (Figures 5e to h). β-catenin staining also changed from cytoplasmic membrane localization in LNCaP and C4-2B cells to nuclear localization in LNCaP-MMP7 and C4-2B-MMP7 cells (Figures 5i to l). Further, Western blot analysis showed that full-length E-cadherin and ZO-1 levels were reduced, while soluble E-cadherin (sE-cadherin, a cleaved fragment that is 40 KDa shorter than the full-length E-cadherin) levels were increased in LNCaP-MMP7 and C4-2B-MMP7 cells, compared to LNCaP and C4-2B cells (Figures 5m and n). Of note, the levels of sE-cadherin were also higher in *Mmp7*$^{+/+}$ and *Mmp7*$^{+/-}$ prostates than *Mmp7*$^{-/-}$ prostates (Figure 4e). As expected, the levels of β-catenin, vimentin, Snail, and Slug were increased in LNCaP-MMP7 and C4-2B-MMP7 cells, compared to LNCaP and C4-2B cells (Figures 5m and n). Similar results were obtained from PC-3 and PC-3-MMP7 cells (Supplementary Figure S3f). It has been reported that E-cadherin and β-catenin form a complex,[40] and we confirmed this in LNCaP, C4-2B, and PC-3 cells (Supplementary Figure S3i and j). Together, these results suggested that MMP7 cleaved E-cadherin to release β-catenin from E-cadherin/β-catenin complex, leading to nuclear translocation of β-catenin and subsequently activation of downstream transcription factors Snail and Slug, hence inducing EMT.

MMP7 increases prostate cancer cell invasion

Since EMT is known to promote cancer cell invasion,[41] we assessed if MMP7-induced EMT could promote prostate cancer cell invasion. We found that LNCaP-MMP7, C4-2B-MMP7, and PC-3-MMP7 cells invaded through Matrigel®-coated porous membranes in significantly larger numbers than LNCaP, C4-2B, and PC-3 cells ($P < 0.05$ or 0.01, Figures 6a to d, and Supplementary Figure S3a to e). On the other hand, mouse prostate cancer cells isolated from *Mmp7*$^{-/-}$ prostates invaded through Matrigel®-coated porous membranes in

significantly smaller numbers than mouse prostate cancer cells isolated from *Mmp7*$^{+/+}$ prostates ($P < 0.01$, Figures 6e and f). These results indicated that MMP7 expression increased prostate cancer cell invasion.

IL-17 induces MMP7 to enhance EMT

Since we have previously demonstrated that IL-17 induces MMP7 expression in mouse prostate,[16] we hypothesized that IL-17 could induce MMP7 to enhance EMT. To test this hypothesis, we first assessed EMT markers in RC$^+$ and RC$^-$ mouse prostate tumors. These tumors were developed due to *Pten* KO and differed in either expressing *Il-17rc* (RC$^+$) or not expressing *Il-17rc* (RC$^-$).[16] We found that RC$^-$ prostate tumors had increased expression of E-cadherin, claudin, and ZO-1, but had decreased expression of MMP7, β-catenin, vimentin, and N-cadherin, compared to RC$^+$ prostate tumors by IHC staining (Figures 7a to e; and Supplementary Figures S2e and f). Western blot analysis confirmed the IHC results (Figure 7f). Further, RC$^-$ prostate tumors had reduced expression of Snail, Slug, Twist, and ZEB1, compared to RC$^+$ prostate tumors by IHC staining (Supplementary Figures S2a to d). These results showed that *Il-17rc* KO mice recapitulated the weak EMT characteristics in *Mmp7* KO mice, suggesting existence of IL-17-MMP7-EMT axis. To test this axis, we treated LNCaP and C4-2B cells with recombinant human IL-17 and found that IL-17 indeed induced MMP7 expression in both LNCaP and C4-2B cells (Figure 7g). Although the levels of full-length E-cadherin were little affected by increased MMP7 expression, the levels of sE-cadherin were dramatically increased (Figure 7g). As expected, the levels of β-catenin (in the nuclei), Snail, Slug, and Twist were also increased along with the increase in MMP7 expression (Figure 7g). To verify if MMP7 indeed mediated IL-17's action, we transfected LNCaP and C4-2B cells with either control small interfering RNA (siRNA) or MMP7-specific siRNA and then treated the cells with IL-17. We found that MMP7-specific siRNA knocked down the levels of MMP7 expression induced by IL-17. At the same time, the full-length E-cadherin levels were slightly increased compared to the control siRNA-transfected cells (Figure 7h). In contrast, sE-cadherin levels were dramatically reduced in MMP7-specific siRNA-transfected cells compared to control siRNA-transfected cells (Figure 7h). Further, the levels of β-catenin, Snail, Slug, and Twist were also decreased in MMP7-specific siRNA-transfected cells compared to control siRNA-transfected cells (Figure 7h). Similar results were obtained from PC-3 cells (Supplementary Figure S3g and h). Together, these results indicated that IL-17 induced MMP7 expression in prostate cancer cells to cleave E-cadherin and then release β-catenin to induce EMT transcription factors Snail, Slug, Twist, and ZEB-1, leading to increased expression of mesenchymal markers (vimentin and N-cadherin) and decreased expression of epithelial markers (E-cadherin, claudin, and ZO-1). Therefore, these results supported the existence of IL-17-MMP7-EMT axis in prostate carcinogenesis.

Selective MMP7 inhibitor decreases development of prostate cancer

Pten single knockout male mice were treated with Compound III, a selective MMP7 inhibitor[42] for 5 to 6 weeks. Although there was no significant difference in GU-bloc weight between the control and MMP7 inhibitor treatment groups, the percentage of invasive prostate cancer was significantly less in the MMP7 inhibitor treatment group than the control group (Figure 8a to d). IHC staining showed increased expression of E-cadherin and

ZO-1, but decreased expression of β-catenin, vimentin, Snail, Slug, Twist, and ZEB1 in MMP7 inhibitor treatment group, compared to the control group (Figure 8e to l).

IL-17 mRNA levels are positively correlated with *MMP7* mRNA levels in human normal prostates and prostate tumors

We analyzed the Cancer Genome Atlas (TCGA) data and found that both *IL-17* and *MMP7* mRNA levels were slightly increased in human primary prostate tumors compared to human normal prostates, however, the differences were not statistically significant (Figure 9a and b). Nevertheless, we found that *IL-17* mRNA levels were positively correlated with *MMP7* mRNA levels in human normal prostates and prostate tumors (Figure 9c).

DISCUSSION

Prior to the use of spontaneous cancer models, the role of IL-17 in carcinogenesis was quite controversial.[43,44] IL-17 was proposed to have both pro-tumorigenic role[45,46] and anti-tumorigenic role.[47,48] The discrepancies arose from using nude mice, over-expression of IL-17, or grafting of different tumor types.[49,50] However, using animal models of autochthonous cancer, many independent groups have demonstrated that IL-17 promotes development of colon cancer,[9-12] skin cancer,[13,14] breast cancer,[15] prostate cancer,[16,17] lung cancer,[18,19] and pancreas cancer.[20] IL-17 has been shown to cause marked epithelial hyperproliferative responses and inflammatory infiltrates in a colon cancer model.[9] IL-17 has also been shown to promote chemical-induced inflammation and keratinocyte proliferation in a skin cancer model.[13] IL-17 increases cellular proliferation, decreases apoptosis, and enhances angiogenesis in the animal tumors.[16-18] IL-17 recruits myeloid-derived suppressor cells (MDSCs) and increases the suppressive function of MDSCs on T cells, thus creating an immunotolerant tumor microenvironment.[15,18] A recent study has demonstrated a hematopoietic-to-epithelial IL-17 signaling axis as another important driver of pancreatic carcinogenesis.[20]

The present study provides several lines of evidence to support the existence of IL-17-MMP7-EMT axis in prostate carcinogenesis. First, *Mmp7* KO and *Il-17rc* KO mice showed similar prostate tumor phenotype in *Pten*-null mice. Second, both *Mmp7* KO and *Il-17rc* KO prostates showed similarly weak EMT characteristics compared to wild-type mouse prostates. Third, IL-17 directly induced MMP7 expression in three human prostate cancer cell lines and in *ex-vivo* cultured mouse prostate tissues,[16] and IL-17 induced expression of EMT markers in three human prostate cancer cell lines. Finally, MMP7 knockdown blocked IL-17-induced EMT in three human prostate cancer cell lines, which strongly supports that MMP7 mediates IL-17's action in induction of EMT. In human lung cancer cells, IL-17 activates NF-κB to upregulate ZEB1 expression, thus inducing EMT and enhancing lung cancer cell migration.[51] Our previous study has shown that *Mmp9* (rather than *Mmp7*) is induced by IL-17 to promote tumor cell motility in a mouse model of lung cancer.[19] In two human nasopharyngeal cancer cell lines, IL-17 induces expression of MMP2 and MMP9 through activation of p38 kinase and NF-κB pathways, which is accompanied with decreased full-length E-cadherin and increased vimentin levels.[52] It is not clear whether MMP2 and MMP9 expression plays any role in regulating E-cadherin and vimentin levels in

that study.[52] Nevertheless, our present study clearly shows that MMP7 cleaves E-cadherin into sE-cadherin in both human prostate cancer cell lines and mouse prostate tumors, resulting in disruption of E-cadherin-β-catenin complex and release of β-catenin that activates the downstream EMT transcription factors. Loss of membrane-associated E-cadherin has been shown to trigger β-catenin nuclear localization with subsequent c-Myc expression and cellular proliferation in human colon cancer cells.[53,54] β-catenin signaling also inhibits apoptosis.[55,56] Therefore, it is possible that IL-17-induced MMP7 expression not only triggers EMT through activation of β-catenin signaling, but also promotes cellular proliferation and inhibits apoptosis. Further, VEGFA has been shown to be a direct downstream target gene of β-catenin signaling,[57] thus the observed angiogenesis phenotype may also be linked to MMP7-activated β-catenin signaling.

In summary, our findings demonstrate that IL-17 induces MMP7 expression to disrupt E-cadherin/β-catenin complex and release β-catenin, thus enhancing EMT and tumor cell invasion, which indicates IL-17-MMP7-EMT axis as potential targets for developing new strategies in the prevention and treatment of prostate cancer. Our proof-of-principle animal study showed that a selective MMP7 inhibitor decreased expression of EMT markers and significantly reduced the number of invasive prostate cancer, suggesting that IL-17-MMP7-EMT axis is targetable. We also found that *IL-17* mRNA levels were positively correlated with *MMP7* mRNA levels in human normal prostates and prostate tumors. However, further studies are warranted to assess the prognostic potential of IL-17 and MMP7 in human prostate cancer.

MATERIALS AND METHODS

Mice

Animal study was approved by the Animal Care and Use Committee of Tulane University. *Pten*$^{loxp/loxp}$(*Pten*$^{L/L}$) and PB-Cre4 mice were described previously.[16,33] *Mmp7*$^{-/-}$mice (strain name: B6.129-Mmp7^{tm1Lmm}/J; genetic background: B6.129*C57BL/6J)[32] were obtained from the Jackson Laboratory, Bar Harbor, ME. The breeding strategy for generating *Mmp7*$^{-/-}$ and *Pten* double KO mice is shown in Figure 1a. Tail DNA of 3-week-old pups was used for PCR genotyping and PCR primers are shown in Supplementary Table S1. *Il-17rc* and *Pten* double KO mouse prostates were obtained from our previous study.[16] In a separate experiment, 15 *Pten* single KO male mice[16,33] at 6-week-old were randomized by flipping a coin into treatment group (n = 10) and control group (n= 5). The treatment group was treated daily with 60 mg/kg body weight of Compound III, a highly selective MMP7 inhibitor[42] (a gift from AstraZeneca R&D Mölndal, Mölndal, Sweden). Compound III was first dissolved in dimethylsulfoxide (DMSO), then dissolved in phosphate-buffered saline (PBS) up to 200 μl, and injected intraperitoneally once a day from 6-week-old to 12-week-old. It was pre-established that animals should be included if they survived to 12-week-old and they should be excluded if they died before reaching 12-week-old. Two animals died after about 4 weeks of treatment due possibly to obvious adhesion of peritoneal organs, which were excluded from the analysis. Compound III treatment was discontinued at 11-week-old in 3 animals due to abdominal distention, and these 3 animals survived to 12-week-old and were included in the analysis. The control group was injected intraperitoneally

with equal volume of DMSO dissolved in PBS once a day up to 12-week-old. All animals survived to 12-week-old were euthanized for necropsy.

In Vivo fluorescence imaging

Two nmols of MMPSense™ 750 FAST Fluorescent Imaging Agent (Cat#NEV10168, PerkinElmer, Inc.) were injected into the tail vein of 30-week-old male mice 12 hours prior to imaging using IVIS® Lumina XRMS imaging system (PerkinElmer, Inc.). The animals were anesthetized with XGI-8 gas anesthesia system (PerkinElmer, Inc.) according to the manufacturer's instructions. Appropriate optical filters were set to collect fluorescence signals from both *Mmp7*$^{+/+}$ and *Mmp7*$^{-/-}$ mice side-by-side simultaneously. Immediately after whole animal imaging, animals were euthanized and then the dissected GU-blocs were imaged for fluorescence signals.

Histopathology

Mice were euthanized and weighed at 9, 12, or 30 weeks of age. The GU-blocs were photographed, weighed with an empty bladder, and fixed as described.[16,58] Thirty-two consecutive 4-μm sections of each prostate were cut and eight sections (from every 8th section) per sample were H&E stained for histopathologic assessment in a genotype-blinded fashion according to the Bar Harbor Classification.[58] The prostatic glands were assessed under low- and high-power magnifications, and approximately 17 to 370 prostatic glands in each prostate were counted.

IHC, immunofluorescence, and terminal deoxynucleotidyl transferase dUTP nick end labeling (TUNEL) staining

IHC staining was performed according to previously established protocols,[16,17] using VECTSTAIN ABC kits and DAB Substrate Kits (Vector Laboratories, Burlingame, CA) according to the manufacturer's instructions. The primary antibodies used were: rabbit anti-E-cadherin (#3195), anti-β-catenin (#8480), anti-vimentin (#5741), anti-N-cadherin (#13116), anti-claudin-1 (#13255), anti-ZO-1(#8193), anti-Snail (#3879), anti-Slug (#9585), and anti-TCF8/ZEB1 (#3396) (Cell Signaling Technology, Beverly, MA); mouse anti-β-catenin (#05-613) and anti-Ki-67 (#AB9260) (Millipore, Billerica, MA); rabbit anti-VEGFA (#sc-152, Santa Cruz Biotechnology, Dallas, TX); rabbit anti-CD31 (#Ab28364, Abcam, Cambridge, MA); rabbit anti-laminin (#L9393, Sigma-Aldrich, St. Louis, MO); goat anti-MMP7 (#AF2967, R&D Systems, Minneapolis, MN). For immunofluorescence staining, monolayer cultured cells were fixed in methanol and blocked with 5% normal donkey serum in PBS; the cells were incubated with anti-E-cadherin or anti-β-catenin antibodies overnight at 4°C; after 3 washes, the cells were incubated with Cy™3-conjugated anti-mouse IgG (#715-485-150) or DyLight™488-conjugated anti-rabbit IgG (#711-485-152, Jackson ImmunoResearch Laboratories, West Groove, PA) for 1 hour at room temperature; and the nuclei were stained with Hoechst33342. TUNEL staining was performed using TACS.XL® Blue Label In Situ Apoptosis Detection Kits (Trevigen, Gaithersburg, MD) according to the manufacturer's instructions. Quantification of the staining was performed as previously described.[16,17]

Cell Culture

Human prostate cancer cell lines (LNCaP, C4-2B, and PC-3) were authentic and free of mycoplasma as described previously[59] and cultured in monolayer in a humidified 5% CO_2 incubator at 37°C. The cell lines were transfected with human MMP7 plasmid (Addgene, Cambridge, MA, USA) using Lipofectamine® 2000 Transfection Reagent (Invitrogen, Grand Island, NY, USA) according to the manufacturer's instructions. Positive cells were selected with 1 mg/ml Geneticin® (Invitrogen) for two weeks and the cells stably overexpressing MMP7 were named LNCaP-MMP7, C4-2B-MMP7, PC-3-MMP7, respectively. The cells were treated without or with 20 ng/ml recombinant human IL-17 (R&D Systems) for 0.5, 2, and 8 hours. In another experiment, the cells were first transfected with 5 nM control siRNA (catalog #4390843, Silencer® Select Negative Control) or 5 nM siRNA targeting MMP7 (catalog #4392420, Silencer® Select Pre-designed siRNA) (Fisher Scientific) using Lipofectamine® 2000 Transfection Reagent (Invitrogen) according to the manufacturer's instructions; 24 hours later, the cells were treated without or with IL-17 for 2 and 8 hours.

Western Blot Analysis

Mouse prostate tissues and cultured cells were homogenized for protein isolation. For IL-17-treated cells, nuclear protein was isolated for detecting nuclear β-catenin, using ProteoExtract® Subcellular Proteome Extraction kit (Millipore) according to manufacturer's instructions. Whole cell lysate was used for detecting other proteins as described previously.[60]

Invasion Assay

Invasion assay was performed using Corning® BioCoat™ Matrigel® Invasion Chambers (Corning Inc., Corning, NY) following the manufacturer's instructions. Approximately 2×10^5 cells (human prostate cancer cells and mouse prostate cancer cells isolated from *Mmp7*$^{+/+}$ and *Mmp7*$^{-/-}$mice) were seeded in the upper chamber in serum-free medium in triplicate wells per group, while the lower chamber contained medium with 10% FBS; 48 and 72 hours later, non-invaded cells were removed from the upper chamber with a cotton swab; the cells invaded through the Matrigel®-coated porous membrane were fixed with methanol, stained with 0.5% crystal violet, and counted under a microscope.

Immunoprecipitation

Whole cell lysates were used for immunoprecipitation (IP) and Western blot (WB) using control IgG, anti-β-catenin, or anti-E-cadherin antibodies, according to our previously described protocol.[61]

The Cancer Genome Atlas (TCGA) Data Analysis

Complete Clinical Dataset (level 2) and RNASeqV2 gene expression dataset (level 3) under the category of human prostate adenocarcinoma (PRAD) were downloaded from the TCGA website https://tcga-data.nci.nih.gov/tcga/. TCGA aligned the sequencing reads using the MapSplice software[62] and quantified expression with upper quartile normalized RNASeq by Expectation Maximization (RSEM) count estimates.[62,63] The mRNA expression dataset

contains 52 normal prostate tissues and 497 primary prostate tumors. Samples without IL-17 expression data were first filtered out and the remaining normal prostates (N = 29) and prostate tumors (N = 183) were analyzed. Log2 transformation was applied to gene expression levels. The differences of IL-17 and MMP7 expression levels between normal prostates and primary tumors were evaluated using the Student's *t* test. Pearson's correlation analysis was performed between the expression levels of IL-17 and MMP7.

Statistical Analysis

Statistical analysis was performed using the R package "stat" (https://www.r-project.org/). All *in vitro* experiments were replicated three times. Sample sizes were selected on the basis of preliminary results to ensure an adequate power and animal number estimate was based on our previous studies.[16,17] The examiners were blinded to the grouping of animals when assessing the outcomes. Quantitative data are presented as mean ± standard error of the mean (SEM, error bar). Comparisons of the GU-bloc weight and other quantitative data were analyzed using Student's *t* test (two-sided) with the assumption of normal distribution of data and similar variance between the groups. The χ^2 test was used to compare the incidences of PIN and invasive adenocarcinoma. Statistical significance was defined as $P < 0.05$.

Supplementary Material

Refer to Web version on PubMed Central for supplementary material.

ACKNOWLEDGMENTS

ZY was partially supported by National Institutes of Health (R01CA174714 and P20GM103518), Department of Defense (W81XWH-14-1-0050, W81XWH-14-1-0149, W81XWH-14-1-0458 (PI: Feng Chen; Co-I: ZY), and W81XWH-15-1-0444), the Developmental Fund of Tulane Cancer Center (TCC), Louisiana Cancer Research Consortium (LCRC) Fund, and Tulane's Institute of Integrated Engineering for Health and Medicine (TI2EHM). WZ and KZ were partially supported by National Institute on Minority Health and Health Disparities (5G12MD007595, PIs: Gene D'Amour and Guangdi Wang).

REFERENCES

1. Coussens LM, Werb Z. Inflammation and cancer. Nature. 2002; 420:860–867. [PubMed: 12490959]
2. Nickel JC, Downey J, Young I, Boag S. Asymptomatic inflammation and/or infection in benign prostatic hyperplasia. BJU Int. 1999; 84:976–981. [PubMed: 10571623]
3. Gerstenbluth RE, Seftel AD, MacLennan GT, Rao RN, Corty EW, Ferguson K, et al. Distribution of chronic prostatitis in radical prostatectomy specimens with up-regulation of bcl-2 in areas of inflammation. J Urol. 2002; 167:2267–2270. [PubMed: 11956490]
4. Schatteman PH, Hoekx L, Wyndaele JJ, Jeuris W, Van Marck E. Inflammation in prostate biopsies of men without prostatic malignancy or clinical prostatitis: correlation with total serum PSA and PSA density. Eur Urol. 2000; 37:404–412. [PubMed: 10765070]
5. De Marzo AM, Marchi VL, Epstein JI, Nelson WG. Proliferative inflammatory atrophy of the prostate: implications for prostatic carcinogenesis. Am J Pathol. 1999; 155:1985–1992. [PubMed: 10595928]
6. De Marzo AM, Platz EA, Sutcliffe S, Xu J, Gronberg H, et al. Inflammation in prostate carcinogenesis. Nat Rev Cancer. 2007; 7:256–269. [PubMed: 17384581]
7. Sutcliffe S, Platz EA. Inflammation in the etiology of prostate cancer: an epidemiologic perspective. Urol Oncol. 2007; 25:242–249. [PubMed: 17483023]

8. Onishi RM, Gaffen SL. Interleukin-17 and its target genes: mechanisms of interleukin-17 function in disease. Immunology. 2010; 129:311–321. [PubMed: 20409152]
9. Wu S, Rhee KJ, Albesiano E, Rabizadeh S, Wu X, Yen HR, et al. A human colonic commensal promotes colon tumorigenesis via activation of T helper type 17 T cell responses. Nat Med. 2009; 15:1016–1022. [PubMed: 19701202]
10. Chae WJ, Bothwell AL. IL-17F deficiency inhibits small intestinal tumorigenesis in ApcMin/+ mice. Biochem Biophys Res Commun. 2011; 414:31–36. [PubMed: 21939640]
11. Chae WJ, Gibson TF, Zelterman D, Hao L, Henegariu O, Bothwell AL. Ablation of IL-17A abrogates progression of spontaneous intestinal tumorigenesis. Proc Natl Acad Sci U S A. 2010; 107:5540–5544. [PubMed: 20212110]
12. Hyun YS, Han DS, Lee AR, Eun CS, Youn JH, Kim HY. Role of IL-17A in the development of colitis-associated cancer. Carcinogenesis. 2012
13. Xiao M, Wang C, Zhang J, Li Z, Zhao X, Qin Z. IFNgamma promotes papilloma development by up-regulating Th17-associated inflammation. Cancer Res. 2009; 69:2010–2017. [PubMed: 19244111]
14. Wang L, Yi T, Zhang W, Pardoll DM, Yu H. IL-17 enhances tumor development in carcinogen-induced skin cancer. Cancer Res. 2010; 70:10112–10120. [PubMed: 21159633]
15. Novitskiy SV, Pickup MW, Gorska AE, Owens P, Chytil A, Aakre M, et al. TGF-beta Receptor II Loss Promotes Mammary Carcinoma Progression by Th17 Dependent Mechanisms. Cancer Discov. 2011; 1:430–441. [PubMed: 22408746]
16. Zhang Q, Liu S, Ge D, Xue Y, Xiong Z, Abdel-Mageed AB, et al. Interleukin-17 promotes formation and growth of prostate adenocarcinoma in mouse models. Cancer Res. 2012; 72:2589–2599. [PubMed: 22461511]
17. Zhang Q, Liu S, Xiong Z, Wang AR, Myers L, Melamed J, et al. Interleukin-17 promotes development of castration-resistant prostate cancer potentially through creating an immunotolerant and pro-angiogenic tumor microenvironment. Prostate. 2014; 74:869–879. [PubMed: 24691769]
18. Chang SH, Mirabolfathinejad SG, Katta H, Cumpian AM, Gong L, et al. T helper 17 cells play a critical pathogenic role in lung cancer. Proc Natl Acad Sci U S A. 2014; 111:5664–5669. [PubMed: 24706787]
19. Xu B, Guenther JF, Pociask DA, Wang Y, Kolls JK, You Z, et al. Promotion of lung tumor growth by interleukin-17. Am J Physiol Lung Cell Mol Physiol. 2014; 307:L497–508. [PubMed: 25038189]
20. McAllister F, Bailey JM, Alsina J, Nirschl CJ, Sharma R, Fan H, et al. Oncogenic Kras activates a hematopoietic-to-epithelial IL-17 signaling axis in preinvasive pancreatic neoplasia. Cancer Cell. 2014; 25:621–637. [PubMed: 24823639]
21. McAleer JP, Kolls JK. Directing traffic: IL-17 and IL-22 coordinate pulmonary immune defense. Immunol Rev. 2014; 260:129–144. [PubMed: 24942687]
22. Liu C, Qian W, Qian Y, Giltiay NV, Lu Y, Swaidani S, et al. Act1, a U-box E3 ubiquitin ligase for IL-17 signaling. Sci Signal. 2009; 2:ra63. [PubMed: 19825828]
23. Wilson CL, Matrisian LM. Matrilysin: an epithelial matrix metalloproteinase with potentially novel functions. Int J Biochem Cell Biol. 1996; 28:123–136. [PubMed: 8729000]
24. Pajouh MS, Nagle RB, Breathnach R, Finch JS, Brawer MK, Bowden GT. Expression of metalloproteinase genes in human prostate cancer. J Cancer Res Clin Oncol. 1991; 117:144–150. [PubMed: 1848860]
25. Knox JD, Wolf C, McDaniel K, Clark V, Loriot M, Bowden GT, et al. Matrilysin expression in human prostate carcinoma. Mol Carcinog. 1996; 15:57–63. [PubMed: 8561867]
26. Radisky DC. Epithelial-mesenchymal transition. J Cell Sci. 2005; 118:4325–4326. [PubMed: 16179603]
27. Thiery JP, Acloque H, Huang RY, Nieto MA. Epithelial-mesenchymal transitions in development and disease. Cell. 2009; 139:871–890. [PubMed: 19945376]
28. Gilles C, Polette M, Piette J, Birembaut P, Foidart JM. Epithelial-to-mesenchymal transition in HPV-33-transfected cervical keratinocytes is associated with increased invasiveness and expression of gelatinase A. Int J Cancer. 1994; 59:661–666. [PubMed: 7960239]

29. Kang Y, Massague J. Epithelial-mesenchymal transitions: twist in development and metastasis. Cell. 2004; 118:277–279. [PubMed: 15294153]
30. Yang J, Mani SA, Donaher JL, Ramaswamy S, Itzykson RA, Come C, et al. Twist, a master regulator of morphogenesis, plays an essential role in tumor metastasis. Cell. 2004; 117:927–939. [PubMed: 15210113]
31. Yang J, Weinberg RA. Epithelial-mesenchymal transition: at the crossroads of development and tumor metastasis. Dev Cell. 2008; 14:818–829. [PubMed: 18539112]
32. Wilson CL, Heppner KJ, Labosky PA, Hogan BL, Matrisian LM. Intestinal tumorigenesis is suppressed in mice lacking the metalloproteinase matrilysin. Proc Natl Acad Sci U S A. 1997; 94:1402–1407. [PubMed: 9037065]
33. Wang S, Gao J, Lei Q, Rozengurt N, Pritchard C, Jiao J, et al. Prostate-specific deletion of the murine Pten tumor suppressor gene leads to metastatic prostate cancer. Cancer Cell. 2003; 4:209–221. [PubMed: 14522255]
34. Cunningham D, You Z. In vitro and in vivo model systems used in prostate cancer research. J Biol Methods. 2015; 2
35. Nishizuka I, Ichikawa Y, Ishikawa T, Kamiyama M, Hasegawa S, Momiyama N, et al. Matrilysin stimulates DNA synthesis of cultured vascular endothelial cells and induces angiogenesis in vivo. Cancer Lett. 2001; 173:175–182. [PubMed: 11597792]
36. Huo N, Ichikawa Y, Kamiyama M, Ishikawa T, Hamaguchi Y, Hasegawa S, et al. MMP-7 (matrilysin) accelerated growth of human umbilical vein endothelial cells. Cancer Lett. 2002; 177:95–100. [PubMed: 11809536]
37. Noe V, Fingleton B, Jacobs K, Crawford HC, Vermeulen S, Steelant W, et al. Release of an invasion promoter E-cadherin fragment by matrilysin and stromelysin-1. J Cell Sci. 2001; 114:111–118. [PubMed: 11112695]
38. Lochter A, Galosy S, Muschler J, Freedman N, Werb Z, Bissell MJ. Matrix metalloproteinase stromelysin-1 triggers a cascade of molecular alterations that leads to stable epithelial-to-mesenchymal conversion and a premalignant phenotype in mammary epithelial cells. J Cell Biol. 1997; 139:1861–1872. [PubMed: 9412478]
39. Davies G, Jiang WG, Mason MD. Matrilysin mediates extracellular cleavage of E-cadherin from prostate cancer cells: a key mechanism in hepatocyte growth factor/scatter factor-induced cell-cell dissociation and in vitro invasion. Clin Cancer Res. 2001; 7:3289–3297. [PubMed: 11595727]
40. Debelec-Butuner B, Alapinar C, Ertunc N, Gonen-Korkmaz C, Yorukoglu K, Korkmaz KS. TNFalpha-mediated loss of beta-catenin/E-cadherin association and subsequent increase in cell migration is partially restored by NKX3.1 expression in prostate cells. PLoS One. 2014; 9:e109868. [PubMed: 25360740]
41. Tsai JH, Yang J. Epithelial-mesenchymal plasticity in carcinoma metastasis. Genes Dev. 2013; 27:2192–2206. [PubMed: 24142872]
42. Edman K, Furber M, Hemsley P, Johansson C, Pairaudeau G, Petersen J, et al. The discovery of MMP7 inhibitors exploiting a novel selectivity trigger. ChemMedChem. 2011; 6:769–773. [PubMed: 21520417]
43. Martin-Orozco N, Dong C. The IL-17/IL-23 axis of inflammation in cancer: friend or foe? Curr Opin Investig Drugs. 2009; 10:543–549.
44. Zou W, Restifo NP. T(H)17 cells in tumour immunity and immunotherapy. Nat Rev Immunol. 2010; 10:248–256. [PubMed: 20336152]
45. Tartour E, Fossiez F, Joyeux I, Galinha A, Gey A, Claret E, et al. Interleukin 17, a T-cell-derived cytokine, promotes tumorigenicity of human cervical tumors in nude mice. Cancer Res. 1999; 59:3698–3704. [PubMed: 10446984]
46. Numasaki M, Fukushi J, Ono M, Narula SK, Zavodny PJ, Kudo T, et al. Interleukin-17 promotes angiogenesis and tumor growth. Blood. 2003; 101:2620–2627. [PubMed: 12411307]
47. Hirahara N, Nio Y, Sasaki S, Minari Y, Takamura M, Iguchi C, et al. Inoculation of human interleukin-17 gene-transfected Meth-A fibrosarcoma cells induces T cell-dependent tumor-specific immunity in mice. Oncology. 2001; 61:79–89. [PubMed: 11474253]

48. Benchetrit F, Ciree A, Vives V, Warnier G, Gey A, Sautes-Fridman C, et al. Interleukin-17 inhibits tumor cell growth by means of a T-cell-dependent mechanism. Blood. 2002; 99:2114–2121. [PubMed: 11877287]
49. Wang L, Yi T, Kortylewski M, Pardoll DM, Zeng D, Yu H. IL-17 can promote tumor growth through an IL-6-Stat3 signaling pathway. J Exp Med. 2009; 206:1457–1464. [PubMed: 19564351]
50. Kryczek I, Wei S, Szeliga W, Vatan L, Zou W. Endogenous IL-17 contributes to reduced tumor growth and metastasis. Blood. 2009
51. Gu K, Li MM, Shen J, Liu F, Cao JY, Jin S, et al. Interleukin-17-induced EMT promotes lung cancer cell migration and invasion via NF-kappaB/ZEB1 signal pathway. Am J Cancer Res. 2015; 5:1169–1179. [PubMed: 26045995]
52. Wang L, Ma R, Kang Z, Zhang Y, Ding H, Guo W, et al. Effect of IL-17A on the migration and invasion of NPC cells and related mechanisms. PLoS One. 2014; 9:e108060. [PubMed: 25244643]
53. Wu S, Lim KC, Huang J, Saidi RF, Sears CL. Bacteroides fragilis enterotoxin cleaves the zonula adherens protein, E-cadherin. Proc Natl Acad Sci U S A. 1998; 95:14979–14984. [PubMed: 9844001]
54. Wu S, Morin PJ, Maouyo D, Sears CL. Bacteroides fragilis enterotoxin induces c-Myc expression and cellular proliferation. Gastroenterology. 2003; 124:392–400. [PubMed: 12557145]
55. Chen S, Guttridge DC, You Z, Zhang Z, Fribley A, Mayo MW, et al. Wnt-1 signaling inhibits apoptosis by activating beta-catenin/T cell factor-mediated transcription. J Cell Biol. 2001; 152:87–96. [PubMed: 11149923]
56. You Z, Saims D, Chen S, Zhang Z, Guttridge DC, Guan K-l, et al. Wnt signaling promotes oncogenic transformation by inhibiting c-Myc-induced apoptosis. J. Cell Biol. 2002; 157:429–440. [PubMed: 11980918]
57. Easwaran V, Lee SH, Inge L, Guo L, Goldbeck C, Garrett E, et al. beta-Catenin regulates vascular endothelial growth factor expression in colon cancer. Cancer Res. 2003; 63:3145–3153. [PubMed: 12810642]
58. Shappell SB, Thomas GV, Roberts RL, Herbert R, Ittmann MM, Rubin MA, et al. Prostate pathology of genetically engineered mice: definitions and classification. The consensus report from the Bar Harbor meeting of the Mouse Models of Human Cancer Consortium Prostate Pathology Committee. Cancer Res. 2004; 64:2270–2305. [PubMed: 15026373]
59. Li Q, Lambrechts MJ, Zhang Q, Liu S, Ge D, Yin R, et al. Glyphosate and AMPA inhibit cancer cell growth through inhibiting intracellular glycine synthesis. Drug Des Devel Ther. 2013; 7:635–643.
60. Chen C, Zhang Q, Liu S, Parajuli KR, Qu Y, Mei J, et al. IL-17 and insulin/IGF1 enhance adhesion of prostate cancer cells to vascular endothelial cells through CD44-VCAM-1 interaction. Prostate. 2015; 75:883–895. [PubMed: 25683512]
61. Liu S, Zhang Q, Chen C, Ge D, Qu Y, Chen R, et al. Hyperinsulinemia enhances interleukin-17-induced inflammation to promote prostate cancer development in obese mice through inhibiting glycogen synthase kinase 3-mediated phosphorylation and degradation of interleukin-17 receptor. Oncotarget. 2016 doi: 10.18632/oncotarget.7296. [Epub ahead of print].
62. Wang K, Singh D, Zeng Z, Coleman SJ, Huang Y, Savich GL, et al. MapSplice: accurate mapping of RNA-seq reads for splice junction discovery. Nucleic Acids Res. 2010; 38:e178. [PubMed: 20802226]
63. Li B, Ruotti V, Stewart RM, Thomson JA, Dewey CN. RNA-Seq gene expression estimation with read mapping uncertainty. Bioinformatics. 2010; 26:493–500. [PubMed: 20022975]

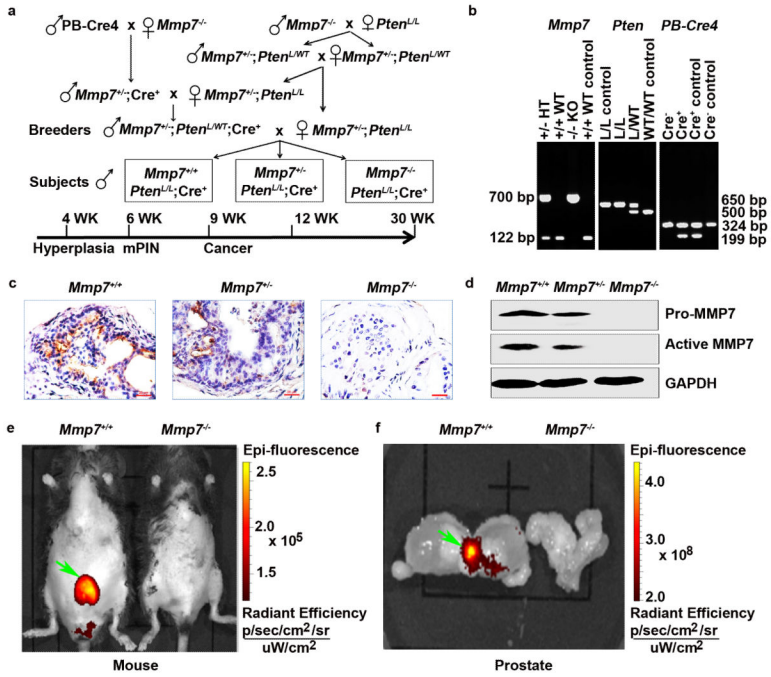

Figure 1.

Establishment of *Mmp7* and *Pten* double KO mouse model. (**a**) Strategy of animal breeding. (**b**) Representative gel images of PCR genotyping. WT, wild-type; HT, heterozygous; KO, knockout. (**c**) IHC staining of MMP7 in dorsal lobes of 30-week-old mouse prostates. (**d**) Western blot analysis of MMP7 protein expression in 30-week-old mouse prostates. (**e**, **f**) Fluorescence imaging of MMP activities in $Mmp7^{+/+}$ and $Mmp7^{-/-}$ mice or mouse prostates. Arrows indicate the fluorescent signals.

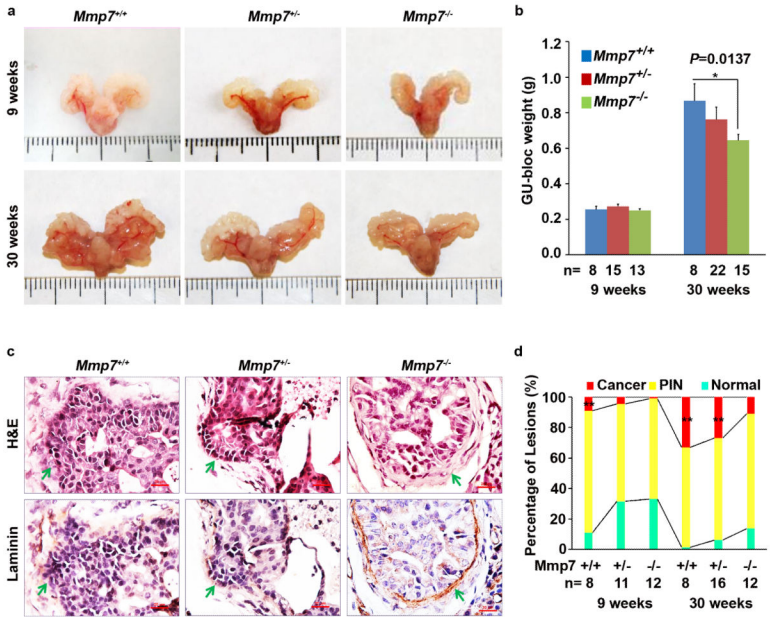

Figure 2.

Mmp7 KO decreases formation of invasive prostate adenocarcinoma in mice. (**a**) Representative photographs of the GU blocs. (**b**) GU-bloc weight. The number of animals in each group is shown under the abscissa. *$P < 0.05$. (**c**) Representative sections of dorsal prostatic lobes stained with H&E or for laminin. Arrows indicate invasive sites in $Mmp7^{+/+}$ and $Mmp7^{+/-}$ mice and non-invasive site in $Mmp7^{-/-}$ mice. (**d**) Percentages of normal, PIN and cancer (invasive prostate adenocarcinoma) in ventral, dorsal, and lateral prostatic lobes at 9 and 30 weeks of age. The number of animals in each group is shown under the abscissa. **$P < 0.01$ compared to $Mmp7^{-/-}$ mice.

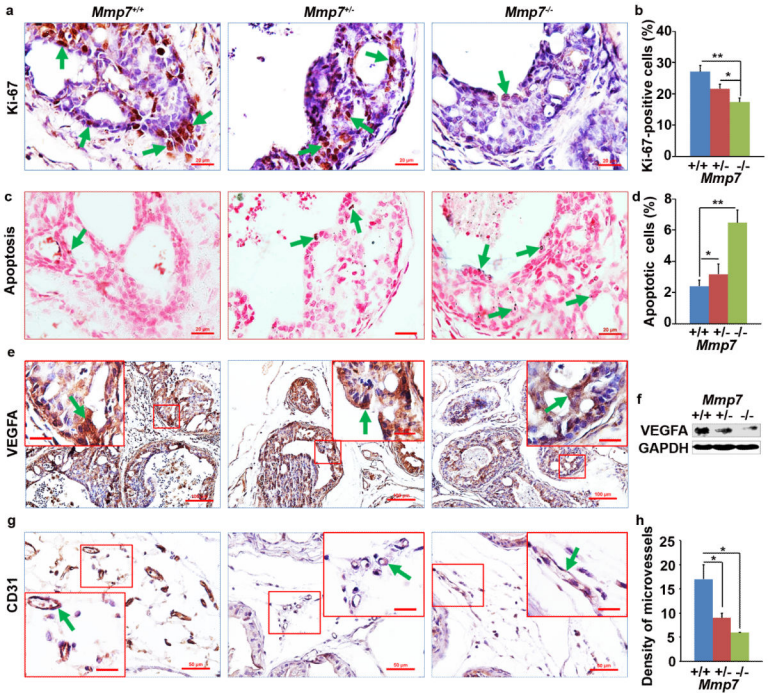

Figure 3.

Mmp7 KO decreases proliferation, increases apoptosis, and inhibits angiogenesis in 30-week-old mouse prostates. (**a**) Representative prostate sections stained for Ki-67. Arrows indicate the positive cells. (**b**) Percentages of Ki-67-positive cells in mouse prostates. Data are represented as mean ± SEM, n = 3 animals per group, $*P < 0.05$ and $**P < 0.01$. (**c**) Representative prostate sections stained for apoptosis (TUNEL assay). Arrows indicate the positive cells. (**d**) Percentages of apoptotic cells in mouse prostates. Data are represented as mean ± SEM, n = 3 animals per group, $*P < 0.05$ and $**P < 0.01$. (**e**) Representative prostate sections stained for VEGFA. Arrows indicate the positive cells. (**f**) Western blot analysis of VEGFA expression in mouse prostates. (**g**) Representative prostate sections stained for CD31. Arrows indicate microvessels. (**h**) Density of microvessels in mouse prostates. Data are represented as mean ± SEM, n = 3 animals per group, $*P < 0.05$.

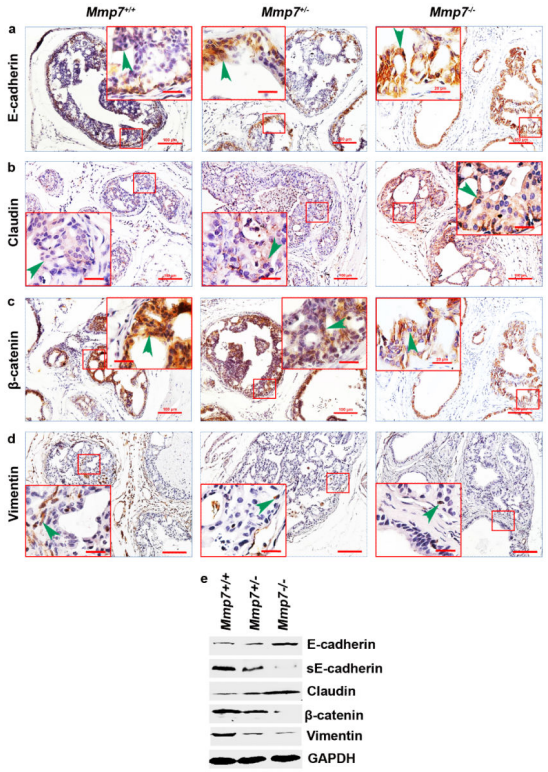

Figure 4.

Mmp7 KO inhibits epithelial-to-mesenchymal transition (EMT) in the prostate lesions in 30-week-old mice. (**a-d**) Representative prostate sections stained for EMT markers. Arrowheads indicate the positive cells. (**e**) Western blot analysis of EMT markers in mouse prostates.

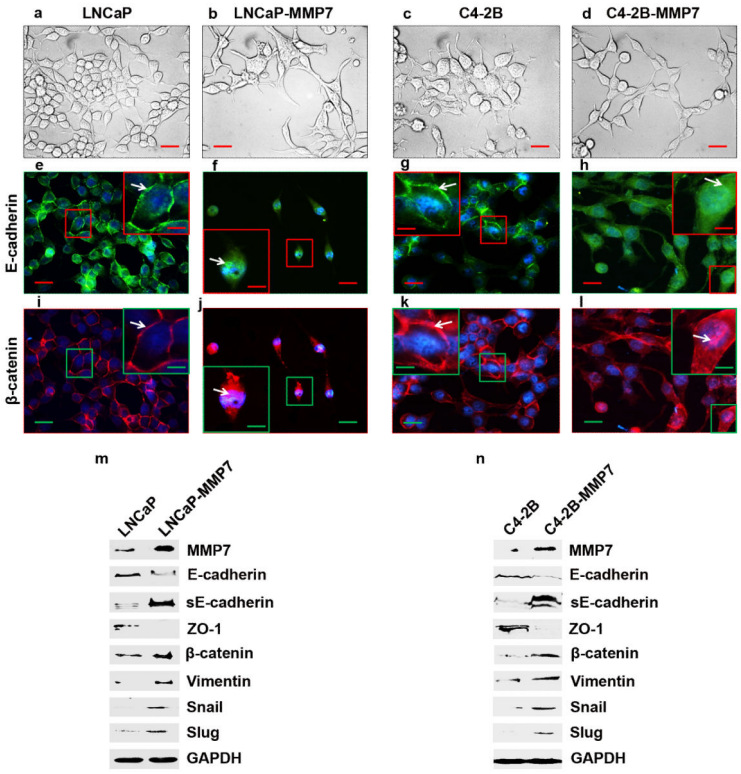

Figure 5.

MMP7 induces EMT in LNCaP and C4-2B cells by disrupting E-cadherin/β-catenin complex. (**a-d**) Phase-contrast photomicrographs of human prostate cancer cells in monolayer culture. (**e-h**) Human prostate cancer cells were stained for E-cadherin (in green color) and the nuclei (in blue color). (**i-l**) Human prostate cancer cells were stained for β-catenin (in red color) and the nuclei (in blue color). (**m-n**) Western blot analysis of EMT markers in human prostate cancer cells.

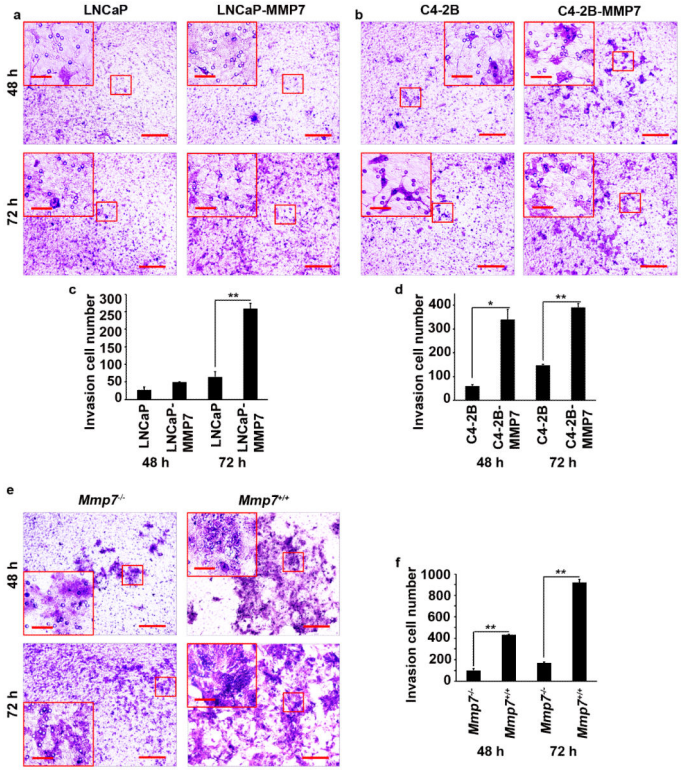

Figure 6.

MMP7 increases prostate cancer cell invasion. (**a-b**) Representative photomicrographs of human prostate cancer cells invaded through the Matrigel®-coated porous membrane. (**c-d**) The number of invasion cells. Data are represented as mean ± SEM, n = 3 wells per group, $*P < 0.05$ and $**P < 0.01$. The experiment was repeated 3 times. (**e**) Representative photomicrographs of mouse prostate cancer cells invaded through the Matrigel®-coated porous membrane. (**f**) The number of invasion cells. Data are represented as mean ± SEM, n = 3 wells per group, $**P < 0.01$. The experiment was repeated 3 times.

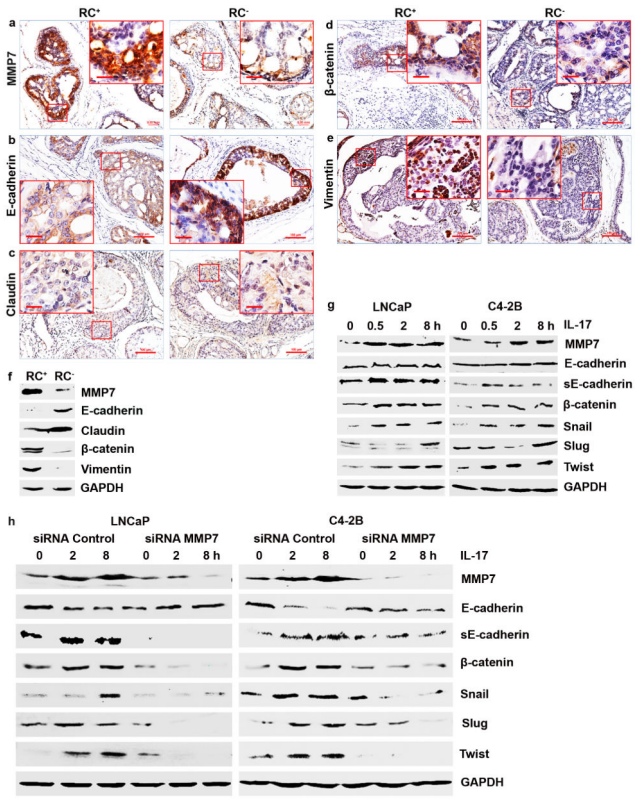

Figure 7.

IL-17 induces MMP7 to enhance EMT. (**a-e**) Representative mouse prostate sections stained for EMT markers. RC^+, *Pten* KO mice expressing IL-17RC. RC^-, *Pten* KO mice not expressing IL-17RC. (**f-h**) Western blot analysis of EMT markers. Of note, the proteins were from either mouse prostate tissue homogenates (**f**) or whole cell lysates (**g, h**), except those used for β-catenin (**g, h**) that were from nuclear extracts.

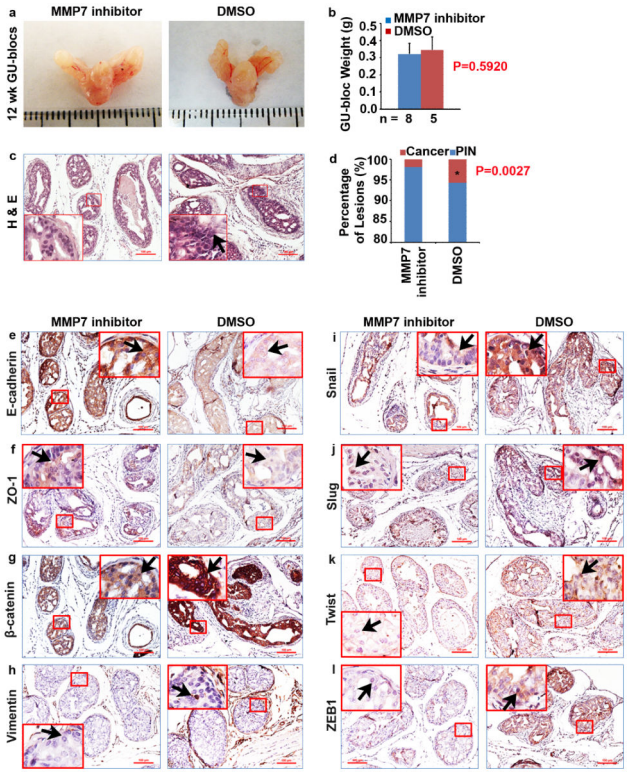

Figure 8.

MMP7 inhibitor decreases formation of invasive prostate adenocarcinoma in mice. *Pten* single conditional KO male mice at 6-week-old were randomized into treatment group (treated with MMP7 inhibitor) or control group (treated with vehicle DMSO); animals were euthanized at 12-week-old. (**a**) Representative photographs of the GU blocs. (**b**) GU-bloc weight. The number of animals in each group is shown under the abscissa. (**c**) Representative sections of dorsal prostatic lobes stained with H&E. Arrows indicate invasive sites in the control group. (**d**) Percentages of PIN and cancer (invasive prostate adenocarcinoma) in ventral, dorsal, and lateral prostatic lobes at 12 weeks of age. (**e-l**) Representative prostate sections stained for EMT markers. Arrows indicate the positive cells.

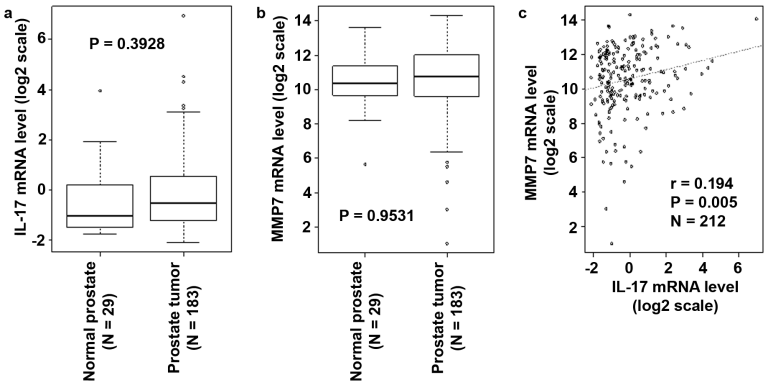

Figure 9.

IL-17 mRNA levels are positively correlated with *MMP7* mRNA levels in human normal prostates and prostate tumors. Complete Clinical Dataset (level 2) and RNASeqV2 gene expression dataset (level 3) under the category of human prostate adenocarcinoma (PRAD) were downloaded from the TCGA website https://tcga-data.nci.nih.gov/tcga/. Log2 transformation was applied to gene expression levels in the included samples. (**a**, **b**) *IL-17* and *MMP7* mRNA levels in normal prostates and primary tumors. (**c**) Correlation between the mRNA levels of *IL-17* and *MMP7*.